

Solids mixing in a circulating fluidized bed

Yu.S. Teplitskii, V.I. Kovenskii*, E.F. Nogotov✱, V.A. Borodulya

A.V. Luikov Heat and Mass Transfer Institute of the National Academy of Sciences of Belarus, 15 P. Brovka Str., Minsk, 220072, Belarus

Received 12 January 2005

Available online 5 June 2006

Abstract

A phenomenological model of solids mixing in a circulating fluidized bed is formulated. The characteristic feature of this model is taking into account the convective flows of particles in the radial direction, which provide the observed in practice essential decrease of the concentration of particles over the riser height. It is established by comparison of calculated and experimental curves of mixing that the value of the coefficient of radial dispersion of particles lies within the range 0.0006–0.006 m²/s.

© 2006 Elsevier Ltd. All rights reserved.

1. Introduction

As is known, solids mixing in the circulating fluidized bed (CFB) is a multifactor process taking place against the background of complicated inner hydrodynamics [1]. For the simulation of the phenomenon various calculation schemes were invoked which reflected, to some extent, the mechanisms of the real process of solids mixing in the CFB apparatuses. The proposed models can be arbitrarily divided into two groups. The first one includes the models of axial (longitudinal) mixing in which the determining quantities and concentrations are considered as depending on just the longitudinal coordinate. In [2], the critical analysis of such models is carried out and on the basis of it a rather simple two-zone model of axial solids mixing is offered which includes the equations:

for the core zone

$$\frac{\partial A\rho_1\bar{c}_1}{\partial t} + u_1 \frac{\partial A\rho_1\bar{c}_1}{\partial x} = \beta_*\rho(\bar{c}_2 - \bar{c}_1) - A\rho_1\beta_1\bar{c}_1; \quad (1)$$

for the annular zone

$$\frac{\partial B\rho_2\bar{c}_2}{\partial t} - u_2 \frac{\partial B\rho_2\bar{c}_2}{\partial x} = \beta_*\rho(\bar{c}_1 - \bar{c}_2) + A\rho_1\beta_1\bar{c}_1. \quad (2)$$

As is shown in [2], this model is able to adequately describe the experimental curves of mixing obtained for both the core zone and the annular zone.

The second group represents the models where the transfer of marked particles in both the axial and radial direction is considered. In [3], the experimental data were interpreted on the basis of the two-dimensional nonstationary model

$$\frac{\partial c^*}{\partial t} = D_a \frac{\partial^2 c^*}{\partial x^2} + \frac{D_r}{r} \frac{\partial}{\partial r} \left(r \frac{\partial c^*}{\partial r} \right) - \frac{\partial(v_s c^*)}{\partial x}, \quad (3)$$

which does not account for the convective motion of particles from the core zone to the annular zone. Probably, that is why the model can be applied only in the upper part of the CFB where the mechanism mentioned above is slackened and the concentrations of particles in both zones are practically independent of the height.

The variation of the density over the CFB height is also not accounted in the model [4]:

$$\frac{\partial(\rho(r)c)}{\partial t} + \frac{\partial(J_s(r)c)}{\partial x} = \frac{D_r}{r} \frac{\partial}{\partial r} \left(r \frac{\partial(\rho(r)c)}{\partial r} \right), \quad (4)$$

where $J_s(r)$ is the value of the local mass flux of particles (positive in the core zone and negative in the annular zone). Model (4) reflects the two-zone structure of CFB and, as

* Corresponding author.

E-mail address: kvi@hmti.ac.by (V.I. Kovenskii).

✱ Deceased.

Nomenclature

A	part of the horizontal section of the riser, occupied by ascending particles (core zone)	Δt_r	time in which particles in the core zone pass through the part of the riser from $x = H_0$ to $x = H$, s
B	part of the horizontal section of the riser, occupied by descending particles (annular zone)	u	superficial gas velocity, m/s
c^*	concentration of marked particles, kg/m ³	u_t	single-particle terminal velocity, m/s
c_1^*, c_2^*	concentrations of marked particles in the core zone and the annular zone, kg/m ³	u_1, u_2	axial velocities of particles in the core zone and the annular zone, m/s
$c = c^*/\rho(r)$	dimensionless concentration of marked particles	u_1^*, u_2^*	radial velocities of particles in the core and annular zone, m/s
$c_1 = c_1^*/\rho_1, c_2 = c_2^*/\rho_2$	dimensionless concentrations of marked particles in the core zone and the annular zone	$u_1' = u_1/(u - u_t), u_2' = u_2/(u - u_t), (u_1^*)' = u_1^*/(u - u_t), (u_2^*)' = u_2^*/(u - u_t)$	
$\bar{c}_1 = \frac{1}{r_0^2} \int_0^{r_0} 2c_1 r dr, \bar{c}_2 = \frac{1}{R^2 - r_0^2} \int_{r_0}^R 2c_2 r dr$	mean dimensionless concentrations of marked particles in the core zone and the annular zone	v_s	velocity of particles, m/s
c_0	initial dimensionless concentration of marked particles	x	vertical coordinate, m
D_a, D_r	coefficients of axial and radial dispersion of particles, m ² /s	$x' = x/H$	
Fr_t	Froude number, $Fr_t = (u - u_t)^2/(gH)$	<i>Greek symbols</i>	
g	free fall acceleration, m/s ²	β_*	coefficient of interphase exchange in (29), 1/s
H	height of the riser, m	β_1	coefficient in (28), 1/s
H_0	height of the bottom fluidized bed, m, $H_0' = H_0/H$	ε	porosity
J_s	mass circulating flow of particles, kg/m ² s	$\rho = A\rho_1 + B\rho_2$	density of the bed mean over horizontal section of the riser, kg/m ³
\bar{J}_s	dimensionless mass flow of particles, $\bar{J}_s = J_s/\rho_s(u - u_t)$	ρ_1, ρ_2	densities of the bed in the core and the annular zone, kg/m ³
$n = \rho_2/\rho_1$		<i>Indices</i>	
Pe	Peclet number, $Pe = (u - u_t)R^2/HD_r$	a	axial
R	radius of the riser, m	c	core
r	radial coordinate, m, $r' = r/R$	d	delay
r_0	radius of the core zone, m, $r_0' = r_0/R = \sqrt{A}$	eff	effective
T	period of circulation, s, $T = \Delta t_r + \Delta t, T' = T(u - u_t)/H$	f	fluid
t	time, s	fb	bottom fluidized bed
t'	dimensionless time, $t' = t(u - u_t)/H$	r	radial
Δt	time of recirculation (time interval between the escape of marked particles from the upper part of the riser and their enter in the riser base), s, $\Delta t' = \Delta t(u - u_t)/H$	s	particles
		t	conditions of floating of a single particle
		0	initial value
		1	core zone
		2	annular zone

well as (3), it can be justifiably used only in the upper part of the bed. Besides, because of the wrong notation of the dispersion term it gives a physically absurd expression $\frac{c_\infty D_r}{r} \frac{\partial}{\partial r} (r \frac{\partial \rho(r)}{\partial r}) \neq 0$ for $t \rightarrow \infty$, when $c \rightarrow c_\infty = \text{const}$. Nevertheless, as the authors of [4] state, this model adequately described the experimental data in the upper part ($x = 4$ m) of the 5-m riser.

As is seen, the field of application of models (3) and (4) is limited. They can be used only in the upper zone of CFB, where $\rho = \text{const}$. Besides, it is important to note that in the models mentioned above there is no evident form of

accounting for the most important mechanism of mixing – radial convection of particles (Fig. 1) which provides the observed in practice essential decrease of ρ_1 and ρ_2 with the height at practically constant longitudinal velocities u_1 and u_2 .

In the present work, two problems were posed: to account for the indicated mechanism of mixing thus increasing the level of theoretical analysis and to develop on this basis the generalized model of the process which describes solids mixing over the whole volume of the riser of CFB.

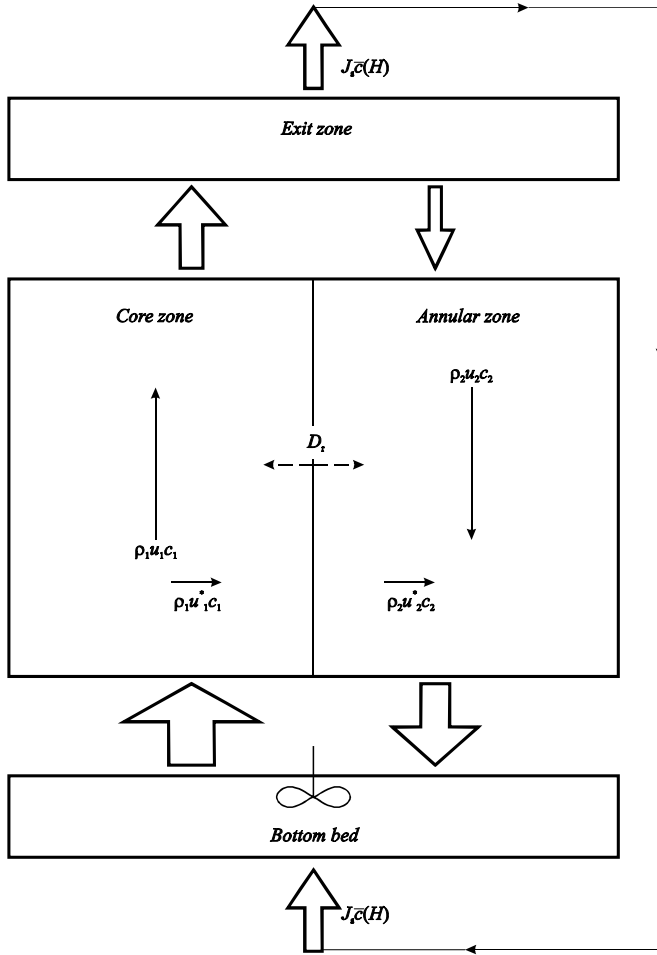


Fig. 1. Model of solids mixing in CFB.

2. Formulation of the theoretical model

Main assumptions which form the basis of the physical model are the following:

- (1) The upward motion of particles with the velocity u_1 in core zone and downward motion near the riser walls with the velocity u_2 (Fig. 1); these velocities are calculated by the formulas

$$u_1 = \frac{u}{A} - u_t, \quad (5)$$

$$u_2 = 0.1(u - u_t)Fr_t^{-0.7}. \quad (6)$$

We note that (5) is written assuming the absence of gas filtration in the annular zone and (6) – according to [5]. In this case, the gas velocity in the core zone is u/A .

- (2) The local densities of the core zone ρ_1 and the annular zone ρ_2 depend only on the longitudinal coordinate x . It is anticipated that there is a linear connection

$$\rho_2 = n\rho_1 \quad (7)$$

between them; here n is a coefficient depending on x (see below).

- (3) In any horizontal section, the equality

$$J_s = Au_1\rho_1 - Bu_2\rho_2 \quad (8)$$

expressing the existence of the outer circulation of particles holds.

- (4) The mean (across the horizontal section) bed density is described by the empirical formula [6]

$$\frac{\rho}{\rho_s} = \bar{J}_s(x')^{-0.82}, \quad H'_0 < x' \leq 1. \quad (9)$$

- (5) The zone with the constant density and almost ideal solids mixing – the bottom fluidized bed – exist in the lower part of the bed. The particles entering from the descending loop and the annular zone are accelerated in this zone of CFB that acts as a peculiar dynamic gas distributor, the height of which depends on the operating parameters of CFB and is calculated by the formula [7]

$$H'_0 = 1.25Fr_t^{-0.8}\bar{J}_s^{1.1}. \quad (10)$$

The porosity of the bottom bed depends weakly on the conditions of CFB operation. In [7], it is offered to calculate this quantity by the relation

$$\varepsilon_{fb} = 1 - 0.33Fr_t^{-0.045}. \quad (11)$$

- (6) Radial convection of particles from the core zone into the annular zone with the velocities u_1^* (core) and u_2^* (annular zone) is taken into account (Fig. 1). It is apparent that the values of these velocities are determined by the rate of changing of the mean CFB density over the riser height (see below).
- (7) The axial transfer of marked particles is disregarded. The possibility of this is discussed in [2].
- (8) The coefficient of radial dispersion of particles in both zones is the same.

As is seen from (7)–(9), there are only two equations for determining the quantities A , B , and n

$$Au'_1 + Bnu'_2 = (A + Bn)(x')^{0.82}, \quad (12)$$

$$A + B = 1. \quad (13)$$

Thus, one of these quantities should be determined beforehand. In [2], it is assumed on the basis of experimental data that $n = 3$ and the quantities A and B are found from (12) and (13) as functions of x . In the present work, for the convenience of numerical calculations, these values are quantities to be constant and equal to: $A = 0.85$, $B = 0.15$, and the quantity n is determined as

$$n = \frac{A u'_1 - (x')^{0.82}}{B u'_2 + (x')^{0.82}}. \quad (14)$$

On the basis of the above assumptions forming the physical model of the process, we write the system of equations of convective dispersion representing the transfer of marked particles in the CFB riser

$$0 \leq r < r_0: \quad \frac{\partial \rho_1 c_1}{\partial t} + u_1 \frac{\partial \rho_1 c_1}{\partial x} + \frac{\rho_1}{r} \frac{\partial}{\partial r} (r u_1^* c_1) \\ = \frac{\rho_1 D_r}{r} \frac{\partial}{\partial r} \left(r \frac{\partial c_1}{\partial r} \right); \quad (15)$$

$$r_0 < r \leq R: \quad \frac{\partial \rho_2 c_2}{\partial t} - u_2 \frac{\partial \rho_2 c_2}{\partial x} + \frac{\rho_2}{r} \frac{\partial}{\partial r} (r u_2^* c_2) \\ = \frac{\rho_2 D_r}{r} \frac{\partial}{\partial r} \left(r \frac{\partial c_2}{\partial r} \right). \quad (16)$$

To determine of radial velocities of particles u_1^* and u_2^* which provide the experimentally observed essential decrease of the bed density over the riser height, we use the equations of continuity of particle fluxes in the corresponding zones:

$$0 \leq r < r_0: \quad \frac{\partial \rho_1}{\partial t} + u_1 \frac{\partial \rho_1}{\partial x} + \frac{\rho_1}{r} \frac{\partial}{\partial r} (r u_1^*) = 0; \quad (17)$$

$$r_0 < r \leq R: \quad \frac{\partial \rho_2}{\partial t} - u_2 \frac{\partial \rho_2}{\partial x} + \frac{\rho_2}{r} \frac{\partial}{\partial r} (r u_2^*) = 0. \quad (18)$$

Based on $\frac{\partial \rho_1}{\partial t} = \frac{\partial \rho_2}{\partial t} = 0$, after integration of (17) and (18) with respect to r we obtain the relations for calculation of the sought-for velocities

$$u_1^* = -\frac{r}{2} u_1 \frac{1}{\rho_1} \frac{d\rho_1}{dx}; \quad (19)$$

$$u_2^* = -\frac{AR^2}{2r} \frac{u_1}{\rho_2} \frac{d\rho_1}{dx} + \frac{1}{2} \left(r - \frac{AR^2}{r} \right) \frac{u_2}{\rho_2} \frac{d\rho_2}{dx}. \quad (20)$$

We note that in deriving (19) and (20) the equality

$$\rho_1 u_1^* = \rho_2 u_2^* \quad \text{at } r = r_0 \quad (21)$$

is used which expresses the condition of continuity of the radial flux of particles on the zone boundary. As is seen from (19) and (20)

$$u_1^*|_{r=0} = 0; \quad (22)$$

$$u_2^*|_{r=R} = -\frac{R}{2\rho_2} \frac{dJ_s}{dx} = 0. \quad (23)$$

Equalities (22) and (23) and the structure of expressions (19) and (20) testify to the physical nature of the obtained dependences for calculation of the velocities u_1^* and u_2^* . The densities of the core zone and the annular zone included in (19) and (20) are expressed in terms of the mean bed density

$$\rho_1 = \frac{\rho}{A + Bn}; \quad \rho_2 = \frac{n\rho}{A + Bn}. \quad (24)$$

It is not difficult to show that Eqs. (1) and (2) describing the axial transfer of the marked particles in CFB are the special case of system (15) and (16). We integrate (15) with respect to r from 0 to r_0 , and (16) – from r_0 to R :

$$\frac{\partial A\rho_1 \bar{c}_1}{\partial t} + u_1 \frac{\partial A\rho_1 \bar{c}_1}{\partial x} + \frac{2r_0 \rho_1}{R^2} (u_1^* c_1) \Big|_{r_0} = \frac{2r_0}{R^2} \rho_1 D_r \frac{\partial c_1}{\partial r} \Big|_{r_0}; \quad (25)$$

$$\frac{\partial B\rho_2 \bar{c}_2}{\partial t} - u_2 \frac{\partial B\rho_2 \bar{c}_2}{\partial x} - \frac{2r_0 \rho_2}{R^2} (u_2^* c_2) \Big|_{r_0} = -\frac{2r_0}{R^2} \rho_2 D_r \frac{\partial c_2}{\partial r} \Big|_{r_0}. \quad (26)$$

In writing (25) and (26) we used equalities (22) and (23) and the condition of the absence of the radial disperse flux of marked particles on the riser wall:

$$\frac{\partial c_2}{\partial r} \Big|_{r=R} = 0. \quad (27)$$

It is assumed formally in (25) and (26)

$$\frac{2r_0}{R^2} \rho_1 (u_1^* c_1) \Big|_{r_0} = A\rho_1 \beta_1 \bar{c}_1; \quad (28)$$

$$\frac{2r_0}{R^2} \rho_1 D_r \frac{\partial c_1}{\partial r} \Big|_{r_0} = \beta_* \rho (\bar{c}_2 - \bar{c}_1). \quad (29)$$

Relationships (28) and (29) express convective and disperse fluxes of marked particles on the zone boundary in terms of the mean concentrations \bar{c}_1 and \bar{c}_2 and thereby determine the effective quantities β_1 and β_* which are the main parameters of the model of axial solids mixing (1) and (2).

Eqs. (1) and (2) follow from (25) and (26) on substitution in them of relationships (28) and (29) in view of the equality

$$\rho_1 \left(u_1^* c_1 - D_r \frac{\partial c_1}{\partial r} \right) \Big|_{r_0} = \rho_2 \left(u_2^* c_2 - D_r \frac{\partial c_2}{\partial r} \right) \Big|_{r_0}, \quad (30)$$

which expresses the continuity of the total flux of the marked particles on the zone boundary. We note that this condition may be named the generalized Dankwerts condition.

By the continuity equations (17) and (18), system (15) and (16) is simplified to

$$\frac{\partial c_1}{\partial t} + u_1 \frac{\partial c_1}{\partial x} + u_1^* \frac{\partial c_1}{\partial r} = \frac{D_r}{r} \frac{\partial}{\partial r} \left(r \frac{\partial c_1}{\partial r} \right); \quad (31)$$

$$\frac{\partial c_2}{\partial t} - u_2 \frac{\partial c_2}{\partial x} + u_2^* \frac{\partial c_2}{\partial r} = \frac{D_r}{r} \frac{\partial}{\partial r} \left(r \frac{\partial c_2}{\partial r} \right). \quad (32)$$

The system of Eqs. (31) and (32), where values of axial and radial velocities of particles are given by Eqs. (5), (6), (19) and (20), reflects the main aspects of the process of solids mixing in CFB and describes the evolution of the associated concentration fields.

We consider two extreme cases:

(a) $D_r \rightarrow 0$. Eqs. (31) and (32) take the form

$$\frac{\partial c_1}{\partial t} + u_1 \frac{\partial c_1}{\partial x} + u_1^* \frac{\partial c_1}{\partial r} = 0; \quad (33)$$

$$\frac{\partial c_2}{\partial t} - u_2 \frac{\partial c_2}{\partial x} + u_2^* \frac{\partial c_2}{\partial r} = 0. \quad (34)$$

As is seen, in this case, the process of mixing is merely convective in nature.

(b) $D_r \rightarrow \infty$. In this case, any difference between the phases is lost. Multiplying (31) by $A\rho_1$, and (32) by $B\rho_2$ and adding the obtained equations, under the condition $c_1 = c_2 = c$ we obtain

$$\rho \frac{\partial c}{\partial t} + J_s \frac{\partial c}{\partial x} = \lim \left(\frac{\rho D_r}{r} \frac{\partial}{\partial r} \left(r \frac{\partial c}{\partial r} \right) \right). \quad (35)$$

The expression $\lim(\frac{\rho D_r}{r} \frac{\partial}{\partial r} (r \frac{\partial c}{\partial r}))$ is an uncertainty of the $\infty \cdot 0$ type. The value of this uncertainty can be found from the condition of physical correspondence of models (1), (2) and (31), (32) for $\beta_* \rightarrow \infty$ and $D_r \rightarrow \infty$, respectively. It is clear that under these conditions the models are bound to describe a common process. In [2], when $\beta_* \rightarrow 0$ the equation

$$\rho \frac{\partial c}{\partial t} + J_s \frac{\partial c}{\partial x} = 0 \quad (35a)$$

was obtained for (1) and (2).

Comparison of (35) and (35a) gives $\lim(\frac{\rho D_r}{r} \frac{\partial}{\partial r} (r \frac{\partial c}{\partial r})) = 0$. Eq. (35a) describes convective transfer of the marked particles with the velocity J_s/ρ .

The obtained system (31) and (32) was used for mathematical modelling of mixing marked particles injected to the bottom fluidized bed at the initial instant of time. We formulate the corresponding boundary conditions.

The initial conditions: $c_1(0, x, r) = c_2(0, x, r) = 0$, $c_1(0, H_0, r) = c_0$;

the boundary conditions:

$$\begin{aligned} r = 0: \quad & \frac{\partial c_1}{\partial r} = 0; \\ r = R: \quad & \frac{\partial c_2}{\partial r} = 0; \\ r = r_0: \quad & u_1^* c_1 - D_r \frac{\partial c_1}{\partial r} = n \left(u_2^* c_2 - D_r \frac{\partial c_2}{\partial r} \right); \\ x = H: \quad & \bar{c}_1 = \bar{c}_2, \\ t \leq T: \quad & H_0 \rho_{fb} \frac{\partial \bar{c}_1}{\partial t} + A \rho_1 u_1 \bar{c}_1 - B \rho_2 u_2 \bar{c}_2 = 0, \\ x = H_0: \quad t > T: \quad & H_0 \rho_{fb} \frac{\partial \bar{c}_1}{\partial t} + A \rho_1 u_1 \bar{c}_1 - B \rho_2 u_2 \bar{c}_2 \\ & = J_s \bar{c}_1(t - \Delta t, H). \end{aligned} \quad (36)$$

For more details about the conditions at $x = H_0$, which reflect the influence of the bottom bed and outer circulation of particles, see [8]. We note that the condition at $x = H$ is a corollary of the relationship

$$A \rho_1 u_1 \bar{c}_1 - B \rho_2 u_2 \bar{c}_2 = J_s (A \bar{c}_1 + B \bar{c}_2), \quad (37)$$

which indicates the presence of inner circulation of particles and the balance of fluxes of marked particles at the outlet from the riser in the presence of good solids mixing in this zone (Fig. 1). From the above it also follows that c_2 at the outlet from the riser ($x = H$) does not depend on the radial coordinate: $c_2(t, H, r) = \varphi(t)$. Similarly, it follows from the condition of ideal particle mixing in the bottom bed that $c_1(t, H_0, r) = \psi(t)$.

Problem (31), (32) and (36) is self-consistent because the concentration of marked particles at the inlet in CFB depends on their concentration at the outlet in the instant of time $t - \Delta t$.

We write the system (31), (32) and (36) in the dimensionless form:

$$\frac{\partial c_1}{\partial t'} + u_1' \frac{\partial c_1}{\partial x'} + (u_1^*)' \frac{\partial c_1}{\partial r'} = \frac{1}{Pe} \frac{1}{r'} \frac{\partial}{\partial r'} \left(r' \frac{\partial c_1}{\partial r'} \right); \quad (38)$$

$$\frac{\partial c_2}{\partial t'} - u_2' \frac{\partial c_2}{\partial x'} + (u_2^*)' \frac{\partial c_2}{\partial r'} = \frac{1}{Pe} \frac{1}{r'} \frac{\partial}{\partial r'} \left(r' \frac{\partial c_2}{\partial r'} \right). \quad (39)$$

The boundary conditions:

$$c_1(0, x', r') = c_2(0, x', r') = 0,$$

$$c_1(0, H_0', r') = c_0;$$

$$r' = 0: \quad \frac{\partial c_1}{\partial r'} = 0;$$

$$r' = 1: \quad \frac{\partial c_2}{\partial r'} = 0;$$

$$r' = \sqrt{A}: \quad (u_1^*)' c_1 - \frac{R}{H} \frac{1}{Pe} \frac{\partial c_1}{\partial r'} = n \left((u_2^*)' c_2 - \frac{R}{H} \frac{1}{Pe} \frac{\partial c_2}{\partial r'} \right);$$

$$x' = 1: \quad \bar{c}_1 = \bar{c}_2,$$

$$\begin{aligned} t' \leq T': \quad & H_0' m \frac{\partial \bar{c}_1}{\partial t'} + \frac{u_2' + (H_0')^{0.82}}{u_1' + u_2'} u_1' \bar{c}_1 \\ & - \frac{u_1' - (H_0')^{0.82}}{u_1' + u_2'} u_2' \bar{c}_2 = 0, \\ x' = H_0': \quad t' > T': \quad & H_0' m \frac{\partial \bar{c}_1}{\partial t'} + \frac{u_2' + (H_0')^{0.82}}{u_1' + u_2'} u_1' \bar{c}_1 \\ & - \frac{u_1' - (H_0')^{0.82}}{u_1' + u_2'} u_2' \bar{c}_2 \\ & = (H_0')^{0.82} \bar{c}_1(t' - \Delta t', 1). \end{aligned} \quad (40)$$

The dimensionless velocities $(u_1^*)'$ and $(u_2^*)'$ entering into (38) and (40) are calculated by formulas

$$(u_1^*)' = 0.41 \frac{r'}{x'} \frac{u_1' u_2'}{u_2' + (x')^{0.82}}, \quad (41)$$

$$(u_2^*)' = 0.41 \frac{1 - (r')^2}{r' x'} \frac{u_1' u_2'}{u_1' - (x')^{0.82}}, \quad (42)$$

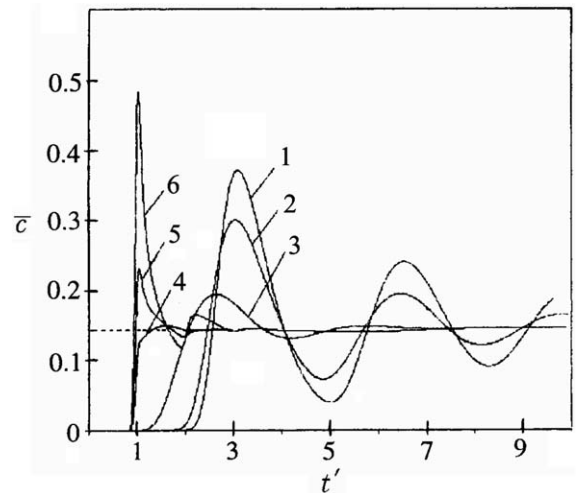


Fig. 2. Dependence of the mean concentration of marked particles on the inlet from the riser on dimensionless time. (1) $Pe = 0.001$; (2) 0.01; (3) 0.1; (4) 1; (5) 5; (6) 500.

which follow from (19) and (20). The quantity $m = \rho_{fb} / \rho(H_0)$ is calculated by the expression $m = 0.4Fr_1^{-0.7}$ obtained from (9)–(11). As is seen, the system (38)–(40) contains an unknown parameter – the coefficient of radial dispersion D_r included in the Pe number.

We estimate the ratio of dispersed and convective radial fluxes of marked particles α . It can be done using Eq. (38) and formula (41):

$$\alpha \approx \frac{x'(u'_2 + (x')^{0.82})}{Pe(r')^2 u'_1 u'_2} \tag{43}$$

Based on $D_r = 0.0025 \text{ m}^2/\text{s}$, $H = 5 \text{ m}$, $R = 0.042 \text{ m}$, $u = 8.2 \text{ m/s}$ and $u_t = 2.3 \text{ m/s}$ (experimental conditions in [4]) for $u'_1 \approx 1$, $u'_2 \approx 0.2$, we obtain $\alpha \approx 6x'(0.2 + (x')^{0.82}) / (r')^2$. Despite the fact that the quantity D_r is somewhat arbitrary, we can draw inference about the significant influence

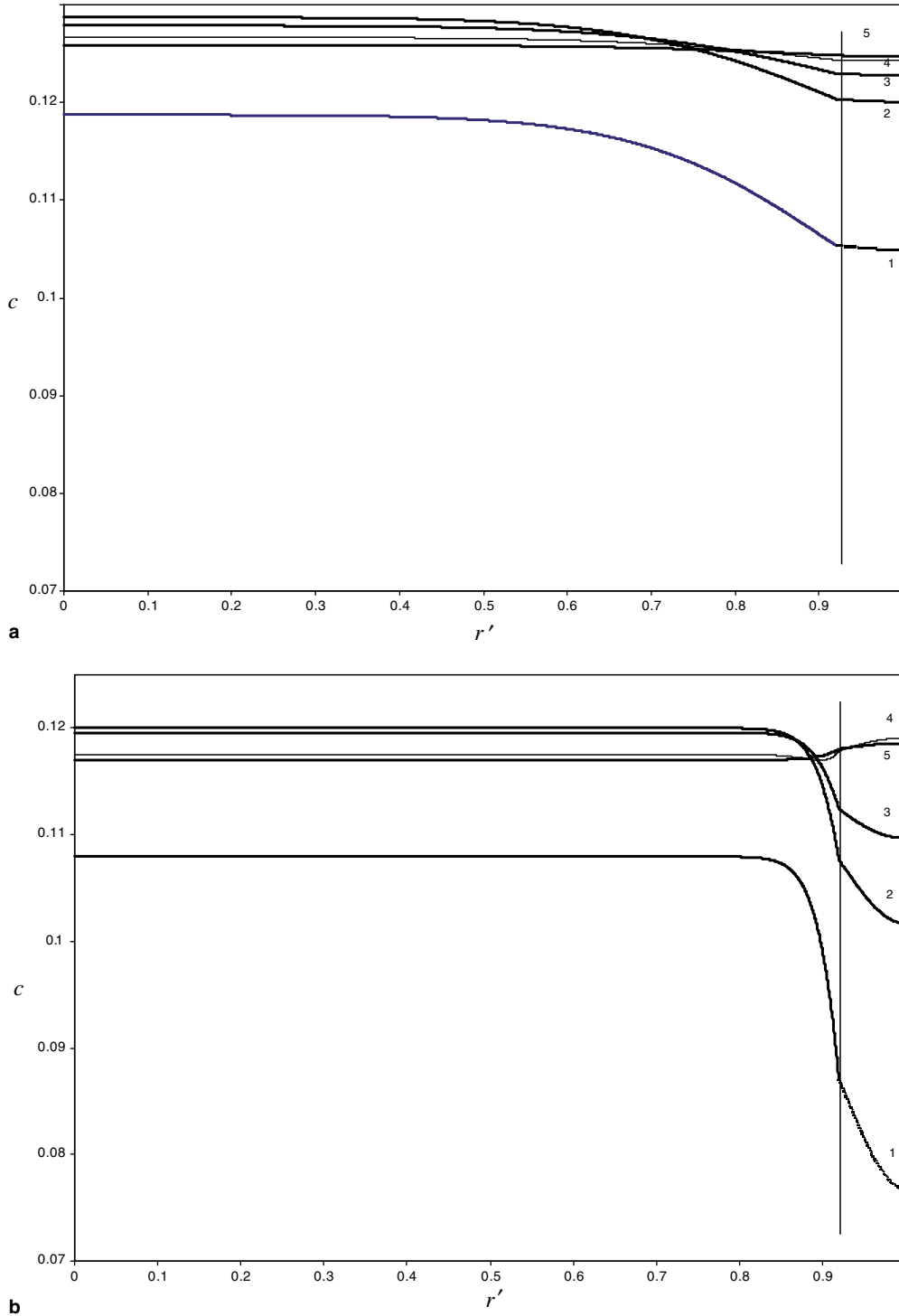


Fig. 3. Dependence of the marked particle concentration on the radius at a height $x' = 0.5$ in various times for $Pe = 10$ (a) and $Pe = 125$ (b): (1) $t' = 1.2$; (2) 2; (3) 2.5; (4) 3; (5) 4.

of radial convective transfer on the process of solids mixing (especially in the bottom part of the riser on the boundary of the zones).

The system of nonstationary differential equations describing the process of solids mixing in the circulating

fluidized bed is solved numerically by the method of finite differences. Implicit finite-difference scheme of the first order of accuracy with respect to the grid pitch h is used. The system of differential equations is solved by the method of marching.

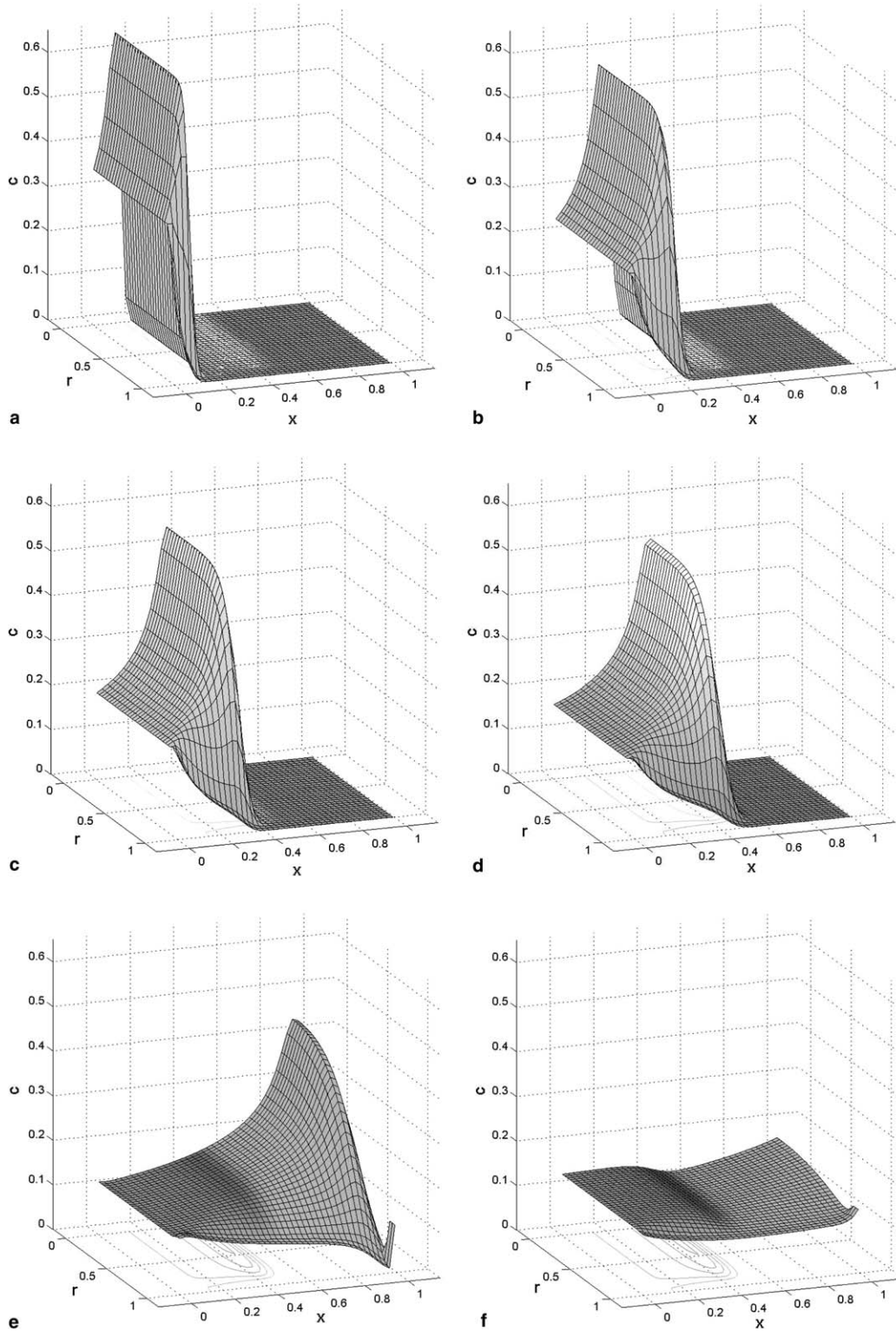


Fig. 4. Evolution of the field of the concentration of marked particles [(a) $t' = 0.1$; (b) 0.2; (c) 0.3; (d) 0.4; (e) 0.8; (f) 1.2; (g) 2] and the fragment of the field for near-wall region at $t' = 0.8$ (h).

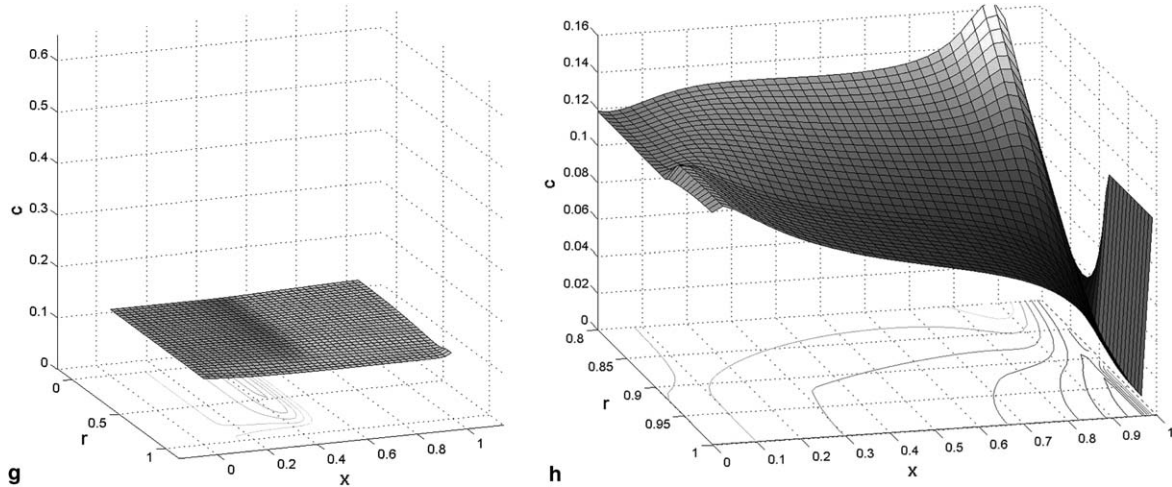


Fig. 4 (continued)

The value of the pitch is chosen in such a way that the solutions received with the step h and $h/2$ differ only from the fourth significant digit. Calculations are stopped on attainment of the stationary regime.

On transition from one time level to the next one the computational algorithm consisted of the following steps:

- (1) the concentration of particles in the bottom bed of the core is calculated;
- (2) successively, going from one space level to another with the step h the distribution of concentration of particles in the central part of the bed (the core) is calculated;
- (3) the value of concentration of particles in the upper part of the annular zone is calculated;
- (4) then, moving from the top down, concentration of particles in the whole annular zone is determined successively, with the step h ;

- (5) the condition of attaining a stationary regime by the solution is checked.

If the condition is not attained, the calculations are repeated from the point 1.

3. The results obtained

Fig. 2 shows the calculation of mean concentrations of marked particles at the outlet from the riser for different values of Pe . Hereafter calculations are made at $H = 12$ m; $u = 6$ m/s; $u_t = 0.5$ m/s; $\rho_s = 2000$ kg/m³; $J_s = 50$ kg/m² s; $\Delta t = 0$ (the marked material is immediately transferred from the outlet point from of the riser to the point of repeated input at $x = H_0$). A stationary value of the concentration c_∞ is calculated by the formula

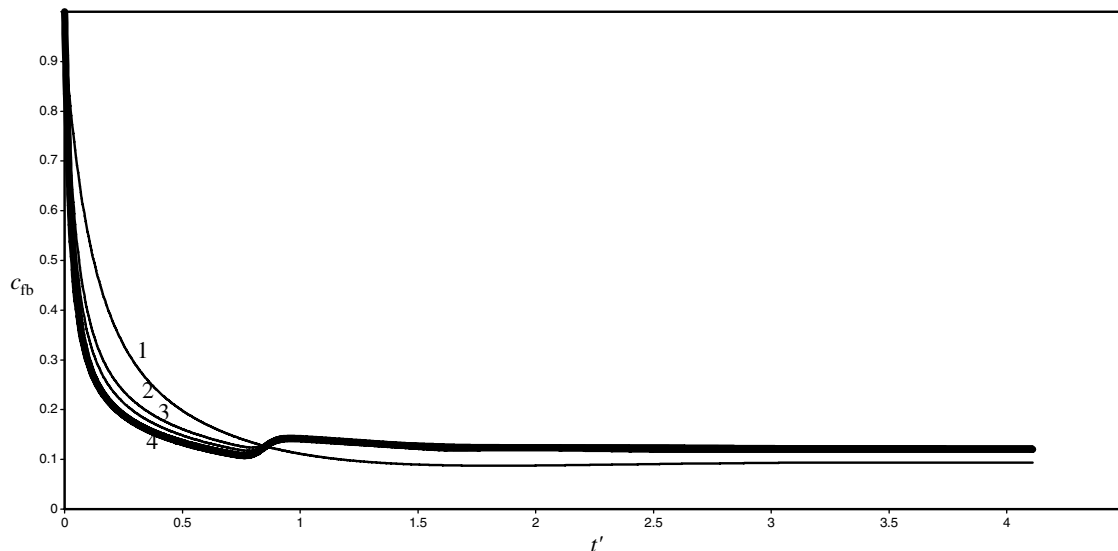


Fig. 5. Dependence of the concentration of marked particles in the bottom bed on time. (1) $Pe = 1$; (2) 5; (3) 10; (4) 50, 500, 5000, 50,000.

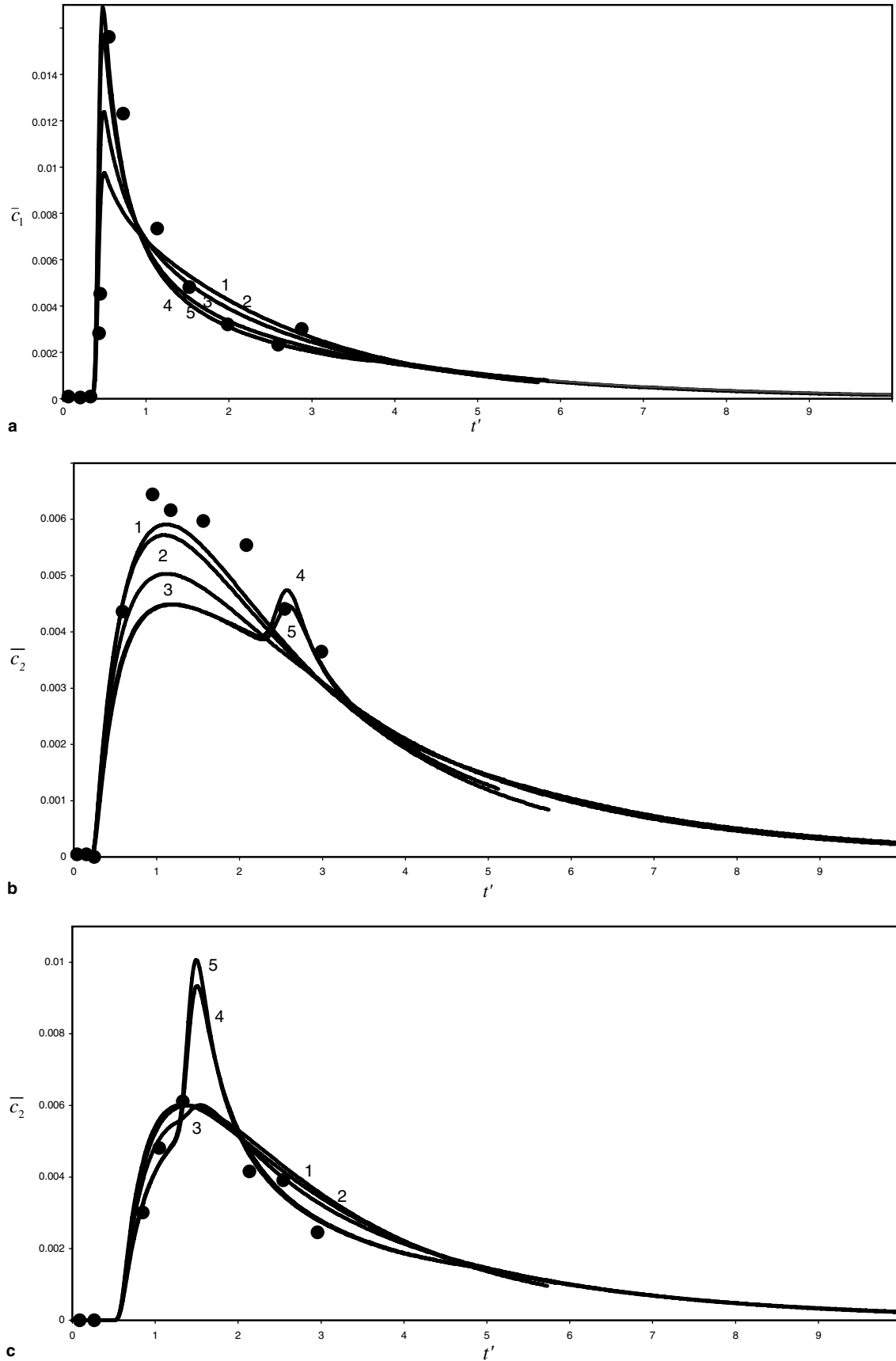


Fig. 6. Comparison of calculational curves of mixing with the experimental data [9] at the height $x' = 0.55$ (a), $x' = 0.32$ (b), $x' = 0.75$ (c): (1) $Pe = 5$; (2) 10; (3) 50; (4) 500; (5) 5000; points – experiment. $c_0 = 0.021$, $J_s = 147 \text{ kg/m}^2 \text{ s}$; $u = 4.57 \text{ m/s}$; $H = 12.2 \text{ m}$.

$$c_\infty = \frac{c_0}{1 + \frac{5.5}{m} \left((H'_0)^{-0.18} - 1 \right)}, \quad (44)$$

which follows from the equation of material balance of the marked particles. Fig. 3 shows the propagation of the concentrations of marked particles along the riser radius at $x' = 0.5$. The influence of the coefficient of radial dispersion D_r on the dependences $c_1(r)$ and $c_2(2)$ is seen well. Fig. 4 shows the detail evolution of the concentration fields in time. The propagation of the wave of the concentration of marked particles in the core zone (at velocity u_1) is clearly defined. The special type of the distribution of the concentration of marked particles at the outlet from the riser (Fig. 4g) corresponds to the condition $\bar{c}_1 = \bar{c}_2$ and reflects the influence of the inner circulation of particles and the equality $c_2(t', 1, r') = \varphi(t')$. The rate of “washing-

out” of the marked particles from the bottom layer is shown in Fig. 5. As is seen, the equilibrium concentration of marked particles is accomplished here at $t' = 1.3$ (at $Pe \geq 1$). Fig. 6 shows the comparison of the calculated for $\Delta t \rightarrow \infty$ experimental data of [9], where the quantities \bar{c}_1 and \bar{c}_2 are measured at different points of the riser with a diameter 0.305 m. The values of D_r obtained by the least square technique is within the range 0.0006–0.006 m²/s. We note that $D_r = 0.0025$ m²/s obtained in [4] is also in the indicated range. We note that peculiar “tongues” in Fig. 6b and c reflect the influence of inner circulation which is clearly seen at low D_r (high Pe). The time of the arrival of these “tongues” is calculated by the formula

$$t_d = \frac{H - H_0}{u_1} + \frac{H - x}{u_2}. \quad (45)$$

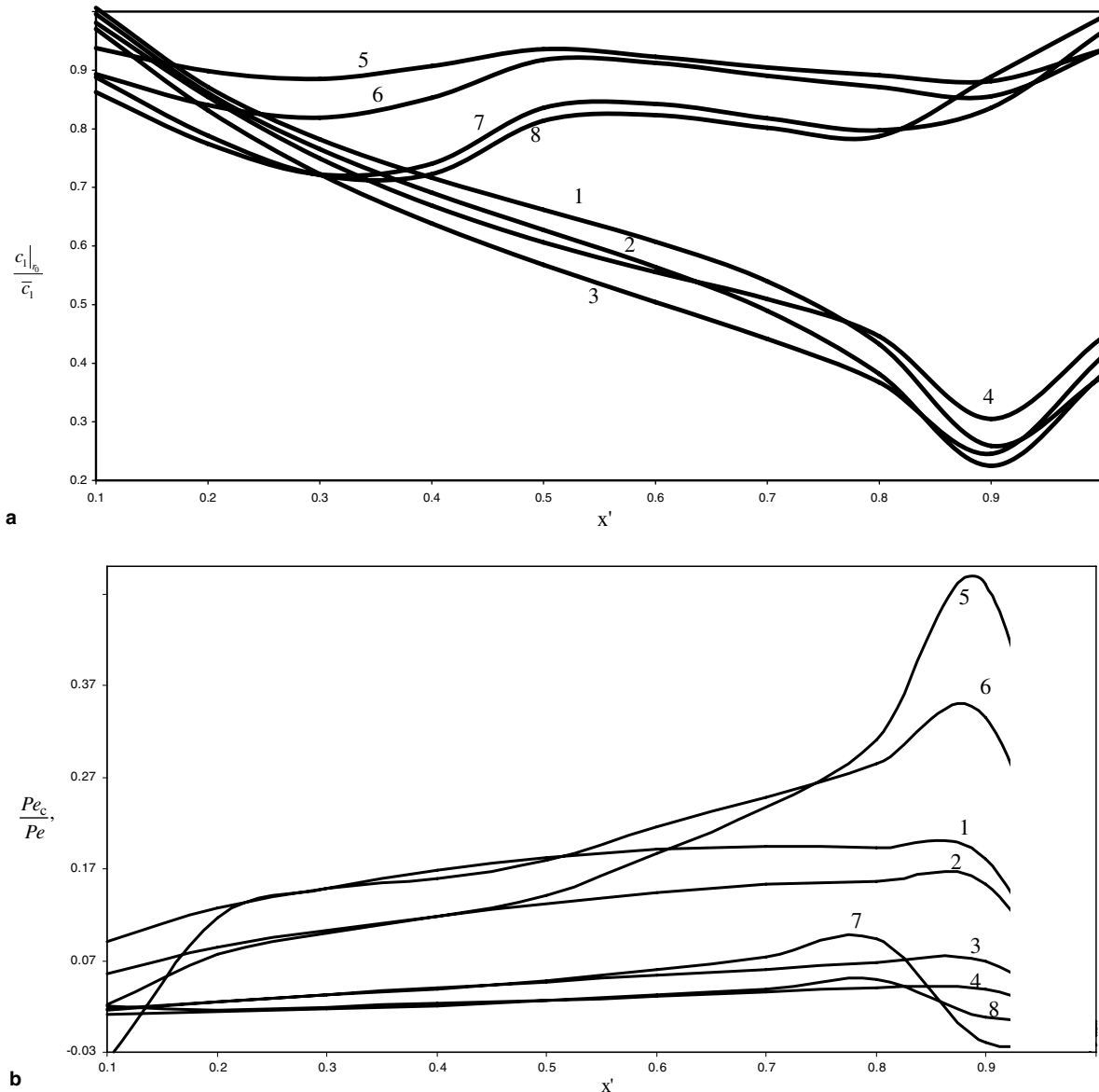


Fig. 7. Dependence of $c_1|_{r_0}/\bar{c}_1$ (a) and Pe_c/Pe (b) on the dimensionless height of the riser: (1, 5) $Pe = 5$; (2, 6) 10; (3, 7) 50; (4, 8) 125; [(1–4) $t' = 0.8$; (5–8) $t' = 1.2$].

From relation (28) we find the equation for the coefficient β_1

$$\beta_1 = -\frac{u_1}{\rho_1} \frac{d\rho_1}{dx} \frac{c_1|_{r_0}}{\bar{c}_1}. \quad (46)$$

In the model of longitudinal mixing [2] this parameter is expressed as

$$\beta_1 = -\frac{u_1}{\rho_1} \frac{d\rho_1}{dx}. \quad (47)$$

In connection with this, of importance is Fig. 7a which shows the quantity $c_1|_{r_0}/\bar{c}_1$ calculated for different heights and times. As is seen, the relation approaches the unity only for relatively large values of time. By analogy, from (29) for β_* we obtain

$$\beta_* = \frac{2D_r}{R^2} \frac{r_0\rho_1}{\rho} \left(\frac{\partial c_1}{\partial r} \Big|_{r_0} / (\bar{c}_2 - \bar{c}_1) \right) \quad (48)$$

or in the dimensionless form

$$\frac{Pe_c}{Pe} = \frac{A + Bn}{2\sqrt{A}} \frac{\bar{c}_2 - \bar{c}_1}{\frac{\partial c_1}{\partial r} \Big|_{\sqrt{A}}}, \quad (49)$$

where $Pe_c = (u - u_i)/(\beta_*H)$. The dependence of Pe_c/Pe on x' at different times is shown in Fig. 7b. As is seen, this quantity is not constant. Fig. 7 attests that model (1) and (2) with the constant coefficient β_* , strictly speaking, is not a result of averaging of (15) and (16). It is defined as an independent model which is able, as the experience implies, in spite of the simplicity, to satisfactorily describe the experimental data.

4. Conclusions

Thus, the formulated generalized model of solids mixing accounts for the main characteristic features of the process:

existence of the inner and outer particle circulation, convective particle fluxes in the radial direction, existence of the bottom bed. The model is able to satisfactorily describe the experimental data and give reasonable values of the coefficient of the radial disperse of particles.

Acknowledgement

This work was carried out with the financial support from the Belorussian Foundation of Basic Research (project No. T02P-071).

References

- [1] A.P. Baskakov, in: V.G. Ainshtein, A.P. Baskakov (Eds.), *Fluidization*, Khimiya, Moscow, pp. 333–395.
- [2] Yu.S. Teplitskii, V.A. Borodulya, E.F. Nogotov, Axial solids in a circulating fluidized bed, *Int. J. Heat Mass Transfer* 46 (2003) 4335–4343.
- [3] F. Wei, Z. Wang, Y. Jin, et al., Dispersion of lateral and axial solids in a cocurrent down-flow circulating fluidized bed, *Powder Technol.* 81 (1994) 25–30.
- [4] G.S. Patience, J. Chaouki, Solids hydrodynamics in the fully developed region of CFB risers, in: *Proceedings of the Eighth Engineering Foundational Conference on Fluidization*, Tours, 1995, vol. 1, pp. 33–40.
- [5] Yu.S. Teplitskii, Near-wall hydrodynamics of a circulating fluidized bed, *Inzh.-Fiz. Zh.* 74 (5) (2001) 177–181.
- [6] V.A. Borodulya, Yu.S. Teplitskii, Scale transition in the circulating bed, in: *Proceedings of Minsk International Forum “Heat and Mass Transfer – MIF-96,”* Minsk, 20–24 May 1996, vol. 5, pp. 69–74.
- [7] Yu.S. Teplitskii, V.I. Kovenskii, Resistance of a circulating fluidized bed, *Inzh.-Fiz. Zh.* 74 (1) (2001) 62–66.
- [8] Yu.S. Teplitskii, Setting of a boundary-value problems of longitudinal solids mixing in circulating fluidized beds, *Inzh.-Fiz. Zh.* 76 (1) (2001) 80–83.
- [9] B. Bader, J. Findlay, T.M. Knowlton, Gas/solids flow patterns in a 30.5-cm-diameter circulating fluidized bed, in: P. Basu, J.F. Large (Eds.), *Circulating Fluidized Bed Technology*, Compeigne, 1988, pp. 123–128.